Performance of a 1.35NA ArF immersion lithography system for 40nm applications

Jos de Klerk[1], Christian Wagner[1], Richard Droste[1], Leon Levasier[1], Louis Jorritsma[1], Eelco van Setten, Hans Kattouw[1], Jowan Jacobs[1], Tilmann Heil[2]

[1]ASML Netherlands B.V.
De Run 6501, 5504 DR Veldhoven, The Netherlands
[2]Carl Zeiss SMT ag
D-73447 Oberkochen, Germany

ABSTRACT

Water based immersion lithography is now widely recognized a key enabler for continued device shrinks beyond the limits of classical dry lithography. Since 2004, ASML has shipped multiple TWINSCAN immersion systems to IC manufacturers, which have facilitated immersion process integration and optimization. In early 2006, ASML commenced shipment of the first immersion systems for 45nm volume production, featuring an innovative in-line catadioptric lens with a numerical aperture (NA) of 1.2 and a high transmission polarized illumination system. A natural extension of this technology, the XT:1900Gi supports the continued drive for device shrinks that the semiconductor industry demands by offering 40nm half-pitch resolution. This tool features a projection lens based on the already proven in-line catadioptric lens concept but with an enhanced, industry leading NA of 1.35. In this paper, we will discuss the immersion technology challenges and solutions, and present performance data for this latest dual wafer stage TWINSCAN immersion system.

Key words: 193nm, high NA, immersion lithography, polarized illumination

1. INTRODUCTION

Soon after the first scanned immersion images in 2003 on the AT:1150i, immersion was mapped out to extend ArF lithography to 40nm and below. In 2006 the first system with a NA larger than 1 was introduced: the XT:1700i with a NA of 1.2 [1]. The XT:1900i is the next step and has a NA of 1.35, the largest NA that is practically possible with water as the immersion liquid. This increase in NA is the key enabler to improve the resolution to 40nm and below.

2. SYSTEM DESCRIPTION

The XT:1900i uses the same design concepts as the XT:1700i and combines the immersion technology of the Twinscan platform with the new very high NA projection system and illumination system. In this way, technological risks are reduced and reliability is improved as is needed for volume production. In this Chapter, the main building blocks, or modules, are described.

2.1. System Overview

The main design aspects are given in the following Table:

	XT:1700i	XT:1900i
NA	1.2	1.35
Lens type	Catadioptric	
Illuminator type	Polarized	
Immersion liquid	Water	
Scan speed [mm/s]	550	600

Table 1. Main design aspects.

This design leads to the following main specifications:

	XT:1700i	XT:1900i
Resolution [nm]	45	40
CD Uniformity [3σ, nm]	2.5	2.0
Dedicated Chuck overlay [99.7%, nm]	6	5
Single Machine Overlay [99.7%, nm]	7	6
Throughput [wafers/hour]	122	131

Table 2. Main specifications.

2.2. Optics

The Starlith™ 1900i is the fifth generation of 193 nm immersion lenses and the second catadioptric lens from Carl Zeiss. This lens provides a NA range of 0.85 to 1.35 and supports field sizes of 26x33 mm^2. The optical design is an inline multiple mirror design and combines the advantages from the refractive and catadioptric designs. The design is characterized by the following properties:

- Rectangular slit with slit height of 26 mm
- Same image orientation as the refractive lens designs to ensure reticle compatibility between existing systems and the high NA systems (no image flip)
- Same high mechanical stability as refractive lens designs
- Low angle of incidence on refractive elements allows standard 193 nm coating technology
- Low angle of incidence on mirrors allows excellent polarization control for s and p states
- Low number of lens elements and more lens manipulators to reduce and control lens heating effects

The Aerial XP™ illuminator supports a wide range of continuously adjustable illumination settings, in different polarization modes and improved pupil parameters as ellipticity and telecentricity. For both polarized and un-polarized usage, the system has maximum efficiency for all supported illumination modes. With the Diffractive Optical Elements (DOE) the partial coherence (σ) range for conventional illumination can be varied between 0.12 and 0.94, for annular illumination the minimum ring width is 0.12 with a maximum sigma value of 0.97, which relates to a geometrical sigma of 1.0.

The key performance parameters for the illumination system are the polarization level and the polarization uniformity on wafer level. The quality of the polarization performance is expressed in the so-called Intensity in the Preferred State (IPS): the ratio of the light intensity in the preferred polarization state and the total intensity. The IPS is measured over the full pupil as function of the field position [2]. As will be shown in the following Chapter, the polarization quality has been improved with respect to the XT:1700i. The improvement has been realized by applying similar lens mounting technology from the Projection lens to the Illuminator lenses. This technology further reduces the stress in the lens elements.

2.3. Immersion Technology

The immersion technology of the XT:1900i is an evolution of the technology used in the XT:1700i. The fluid containment method is based on local containment under the lens using an Immersion Hood (IH). To assure a large working range in resist contact angle at high scan speeds, the ASML scanners use an IH based on a double fluid containment concept. An illustration of the IH concept is given in Figure 1.

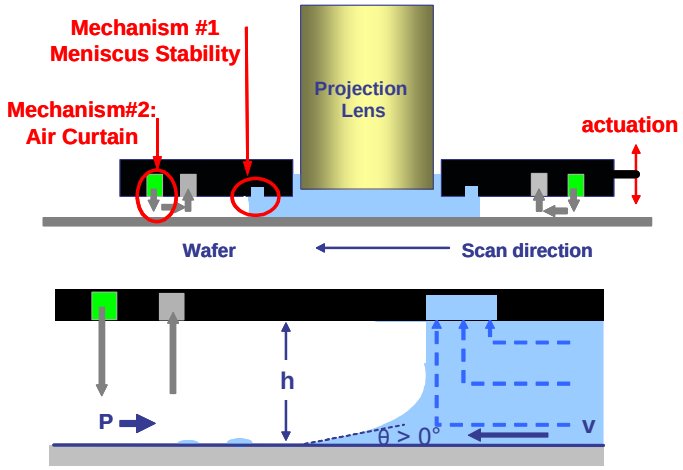

Figure 1. Immersion hood concept with double water containment. The water is independently contained by a meniscus and an air curtain.

The principles of this immersion hood are explained in [1]. In practice the air curtain increases the critical speed and the throughput.

Besides water containment by the immersion hood, thermal control of the wafer is a key aspect of any immersion system. The two most important modules essential for a good thermal control are the immersion hood and the wafer table. In the immersion hood, the uniformity of the laminar water flow has been improved significantly and this results in improved refractive index homogeneity. The wafer table has been improved in two aspects: the spatial thermal control of the wafer and the stability in time. These design improvements yield the Focus and Overlay control as will be presented in the following Chapter.

2.4. Platform Design

All ASML systems have a modular design. This means that platforms are developed that support several lens types and also support both immersion and non-immersion systems. As a result, all systems benefit from improvements in throughput, system dynamics and other aspects. The XT:1900i is build upon a newer platform generation as the XT:1700i and one key improvement of this new platform is the speed of the wafer stages that has been increased from 550 to 600 mm/s.

Furthermore, the high transmissions of the illuminator and projection lens give a throughput that is constant up to exposure doses of 40 mJ/cm^2:

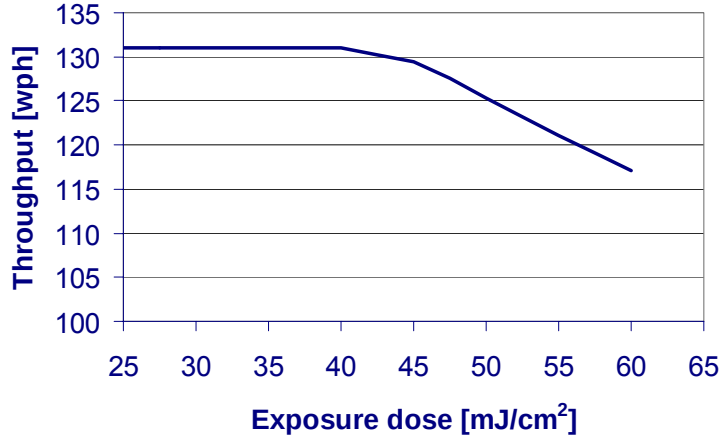

Figure 2. Throughput as function of exposure dose.

Another aspect of this new platform is the improved performance of the interferometer system as used for stage positioning.

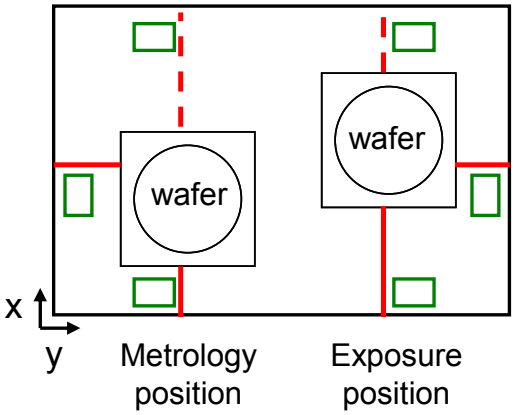

Figure 3. Schematic layout of the stage positioning system. The green boxes are the differential pressure sensors. The red lines are the interferometer bundles and the dotted red lines are the extra beams that are introduced on the new platform. These beams effectively shorten the beam paths hence the effects of environmental disturbances are reduced. In addition, close to each of the six interferometer bundles, so-called differential pressure sensors are placed. These sensors increase the ability to correct faster and more accurate the effect of ambient air pressure variations on the refractive index of the air surrounding the stages.

3. SYSTEM PERFORMANCE

In this chapter the system performance of the system will be presented. The key parameters for lithographic performance are imaging, focus, overlay and productivity. Regarding immersion Defectivity see [3].

3.1. Imaging

3.1.1. Resolution

The ultimate resolution that has been realized is shown in the following Figure with a half pitch of 36.5nm. This corresponds to a k1 value of 0.255 that is very close to the theoretical limit of 0.25. This demonstrates the capability of the 1.35NA lens and means that the image contrast is very high and that contrast contributions like polarization, stray light and dynamics are well under control.

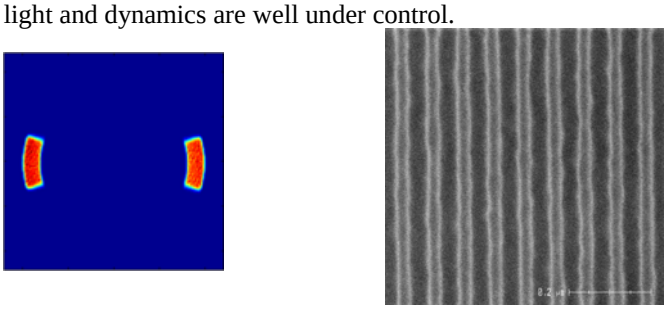

Figure 4. Resist picture of 36.5nm 1:1 dense lines/spaces.

The realized ultimate resolution printing both orientations simultaneously is 37nm as s shown in Figure 5.

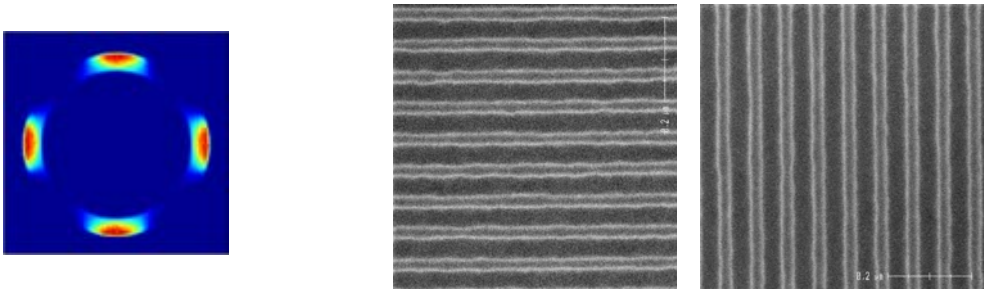

Figure 5. Horizontal and vertical lines of 37nm using C-quad illumination.

The corresponding resist process conditions for showing the system performance are given in the following Table:

Description	Conditions
Photo resist	TOK TArF Pi6001
Thickness	105nm
BARC	83nm ARC 29SR
Topcoat	90nm TCX041
Soft bake temperature	120C
Soft bake time	60 s
PEB temperature	110 C
PEB time	60 s
Developer	Optiyield CD, with prewet against dewetting
Rinse	OptiPattern™ Surface Conditioner
Develop time	60 s

Table 3. Process conditions.

The following Figure shows a large DoF of 720nm for 37nm lines/spaces.

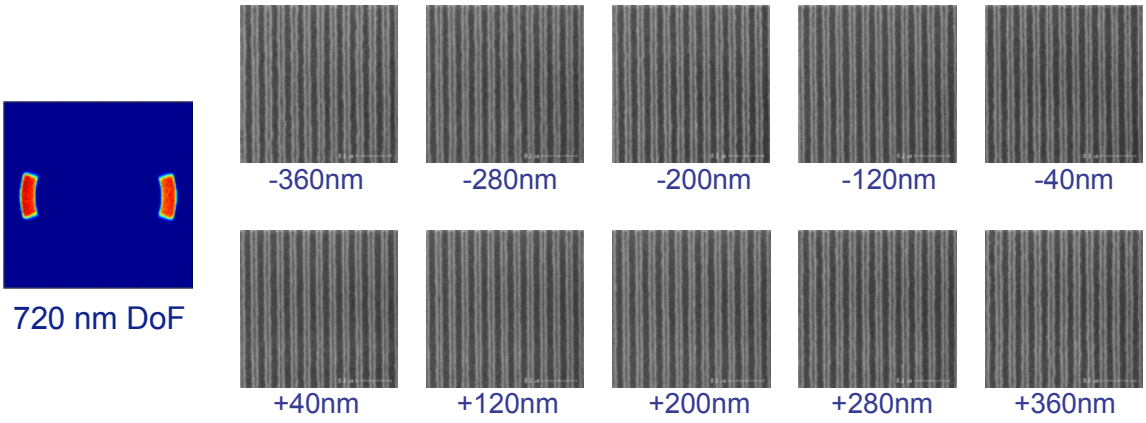

Figure 6. Top down images of 37 nm lines and spaces. Exposed with Dipole Illumination, NA= 1.35.

With the illumination mode called C-quad, both orientations can be printed as is shown in the following Figure.

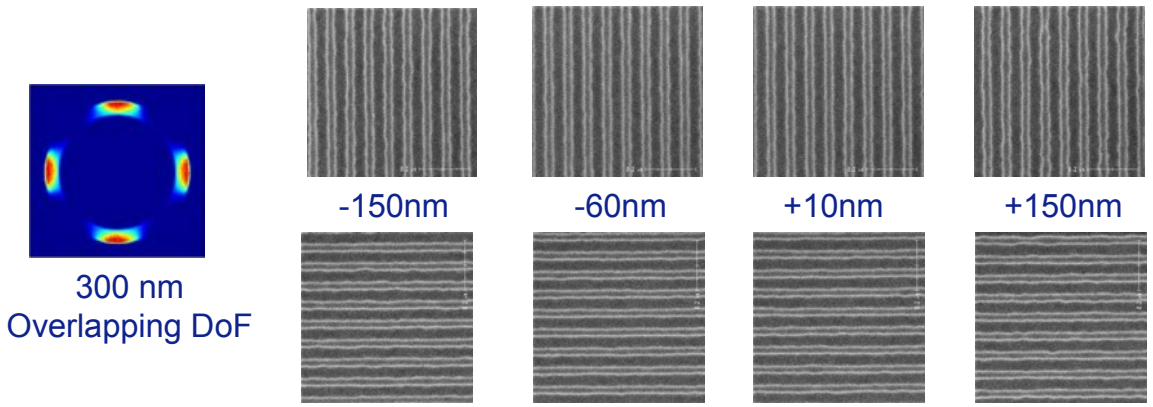

Figure 7. Top down images of 38 nm horizontal and vertical lines and spaces. Exposed with C-quad illumination, NA= 1.35.

Given the Focus control, see Section 3.3, the DoF values are large enough for a robust process window.

3.1.2. CD Uniformity

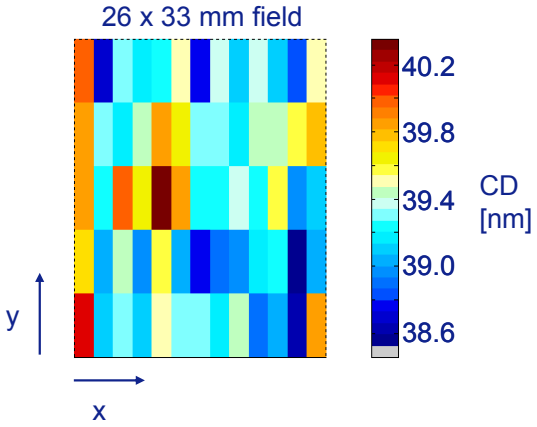

Figure 1. Intra field CD Uniformity of 40nm dense lines/spaces of 1.1nm, 3σ.

The CD Uniformity of 1.1nm could have only been realized because several aspects that contribute to the CD Uniformity are improved, like focus control, as will be shown further on in this chapter.

3.1.3. Projection lens and illuminator performance

As mentioned in the previous Chapter, the XT:1700i and XT:1900i both employ catadioptric lenses. Since many XT:1700i lenses have been produced with Zernike RMS values well below 5 mλ, it is clear that this lens concept is proven.

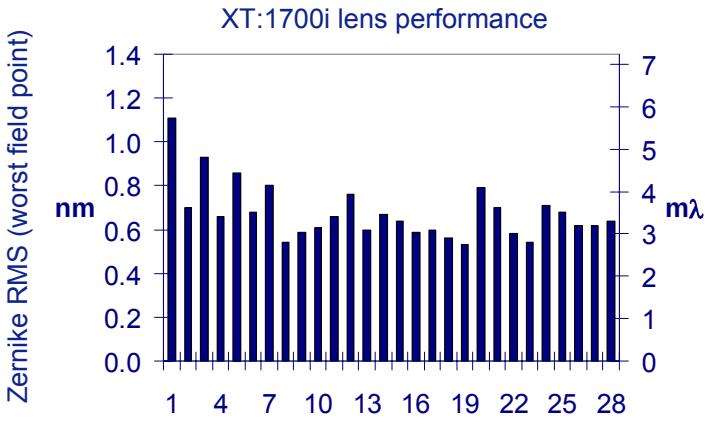

Figure 2. Aberration performance of the XT:1700i with NA=1.2.

The XT:1900i lens performance is shown in the following Figure and includes the grouped Zernike aberrations. As can been seen, the Zernike RMS values are below 4mλ and the grouped Zernikes are below 2 mλ.

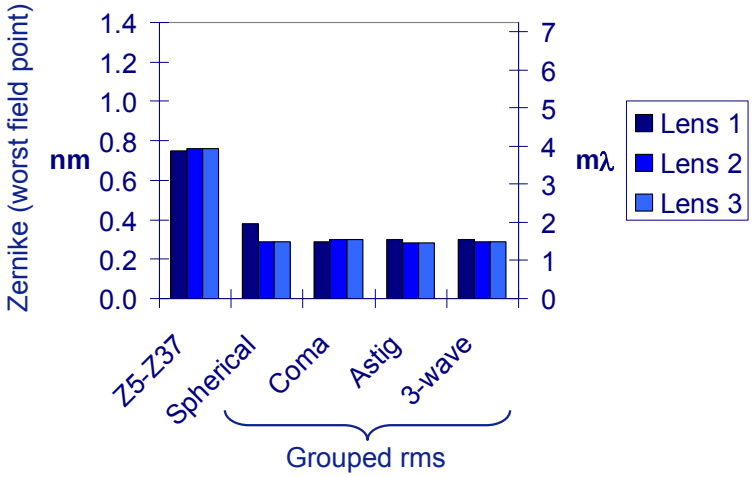

Figure 8. XT:1900i lens aberration performance.

Stray light performance is shown in Figure 9 where the XT:1900i is compared to the average XT:1700i. As can be seen the level is improved by approximately 27%. This has been made possible by improvements of the lens material, coatings and mirror polishing.

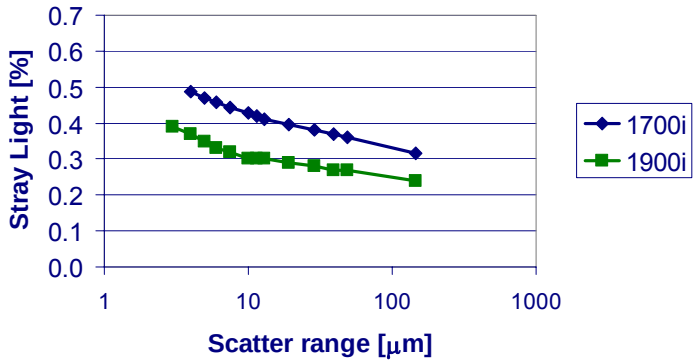

Figure 9. Stray light performance.

Also, the illuminator polarization performance is improved:

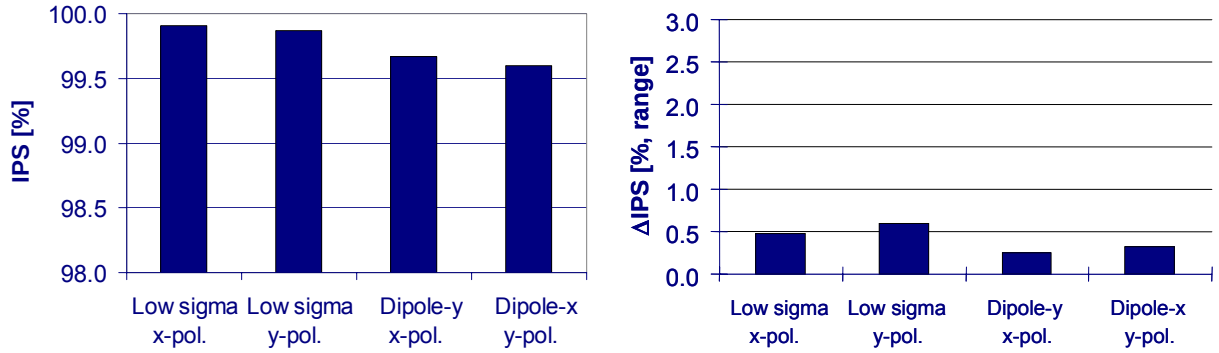

Figure 3. IPS performance (left) and ΔIPS performance (right). The ΔIPS is the IPS variation over the image field.

At these high IPS levels, there is little, if any, image contrast loss and this is one of the improvements leading to a near-perfect resolution as shown in Figure 4.

As is explained in [2], the ΔIPS has a negligible impact on CD Uniformity.

3.2. Lens Heating

The effects of lens heating depend strongly on user applications and conditions like the reticle transmission, the NA, the illumination mode, the exposure dose. In able to control lens heating under these wide variety of conditions, the flexibility to correct lens heating has been made very large, for instance by using many lens manipulators. As an example, an experiment was done on the XT:1700i with 45nm structures. In this experiment, a full wafer lot was exposed with extra dummy exposures to fully saturate the lens. Measurements were done in the beginning and end of the lot. No effects were seen in the DoF. Furthermore, lens heating could induce a change in the best focus difference between different structures, for example by spherical aberration. This has been measured as shown in Figure 10 with a change of the best focus difference of less than 7nm.

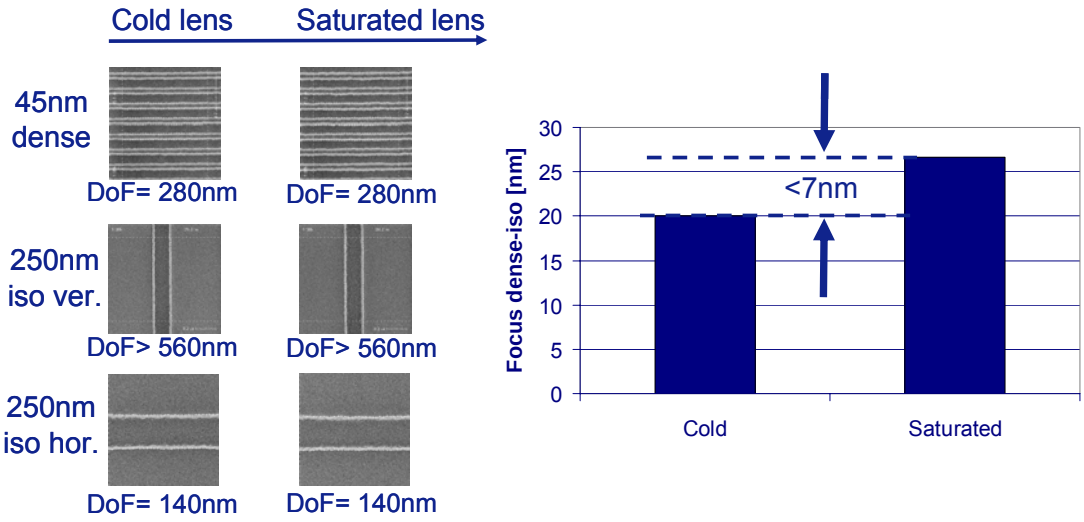

Figure 10. Lens heating experiment of the XT:1700i with Dipole-y illumination and NA=1.2.

For the XT:1900i, the lens transmission has been increased and the manipulator correction ranges have been increased up to factor 2 so a further reduction of lens heating effects can be expected.

3.3. Thermal control

For a good full lot Focus and Overlay control, stable thermal behavior is key, especially in immersion systems. Thermal deviations will deform the wafer leading to Focus and Overlay errors. As a design qualification, this thermal behavior is

measured with special wafers with integrated temperature sensors. The wafer is treated as a normal wafer in the sense that the cycling through the system and the exposure is the same. Three aspects are important for Overlay and Focus: the temperature distribution over the wafers should be uniform, the temperature should be the same for each wafer and the thermal differences between the two wafer chucks should be small. These aspects are measured and visualized in the following Figure.

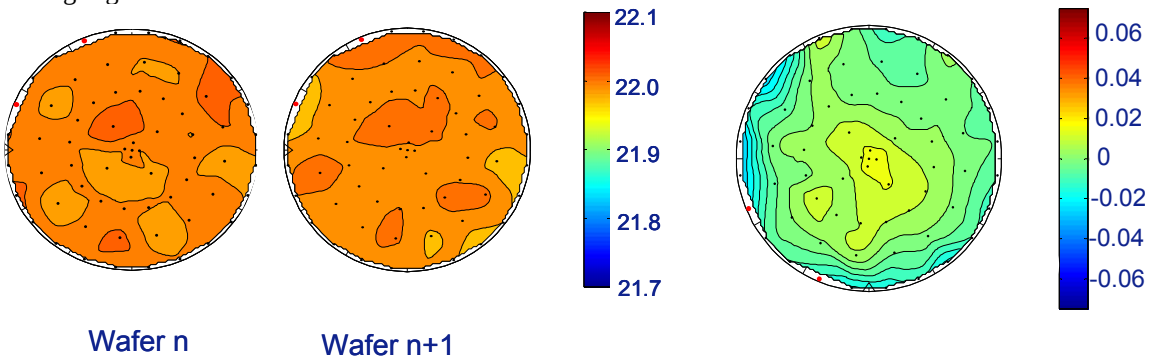

Figure 11. Thermal control of two consecutive wafers (left) and thermal difference between the chucks (right). The scale is in degrees Celcius.

Another important aspect of thermal control is the temperature stability of the water in the immersion hood. The measurement is shown in the following Figure:

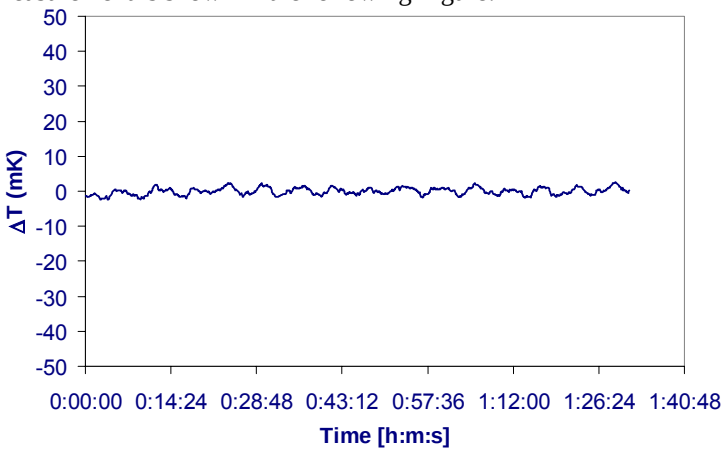

Figure 12. Water temperature stability is within ±2.5 mK over a long period of time.

3.4. Focus performance

Focus performance is measured by the Leveling Verification Test (LVT) and this test measures the full wafer focus control. The uniform thermal wafer control as described in the previous Section results in the full wafer focus control as shown in the following Figure. Another advantage of the stable thermal control is the insensitivity to different wafer exposure layouts, for example different field sizes.

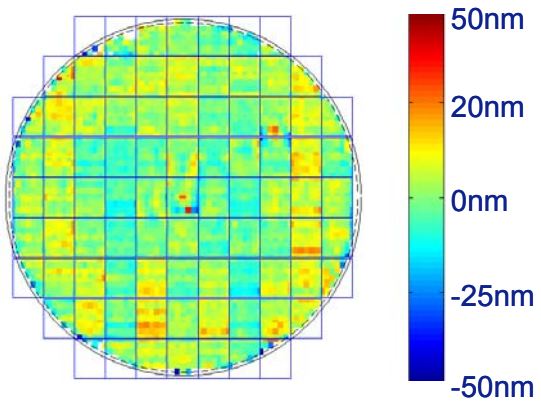

Figure 13. Full wafer focus control of 23nm, 3σ, as measured with the Leveling Verification Test (LVT).

The 3-day focus stability is shown in and includes both wafer stages.

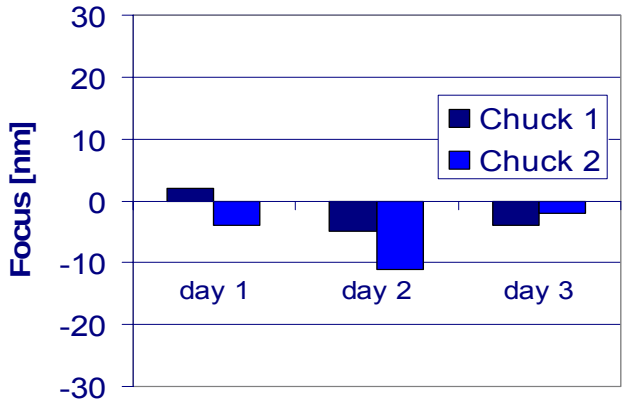

Figure 14. Three day focus stability <13nm.

The Projection Lens Image Plane Deviation (IPD) and Lens Astigmatism are shown in the following graph:

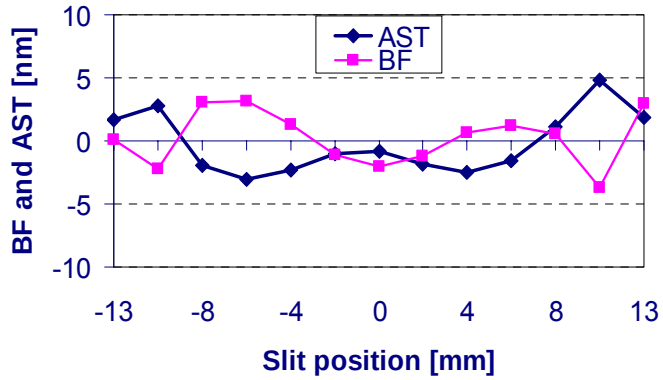

Figure 15. Lens Image Plane Deviation of 11nm and Lens Astigmatism of 5nm.

3.5. Overlay

First, the effect of the uniform laminar water flow in the immersion hood is made visible in Figure 16. The more or less random residuals are caused by thermal effects of the water. The numbers are within the measurement noise and this indicates such a uniform and stable water flow that the immersion hood is virtually absent.

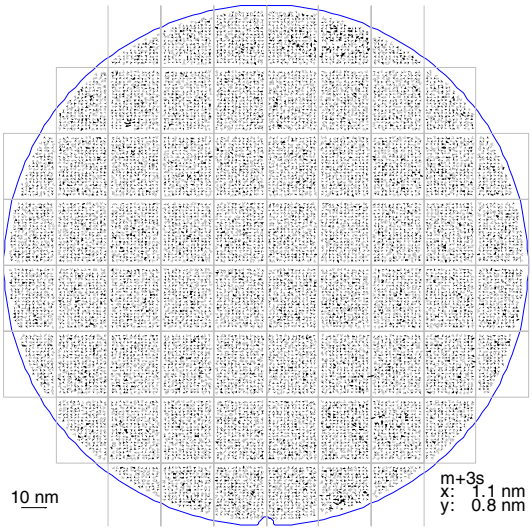

Figure 16. Overlay effects on the uniform water flow in the immersion hood. In this result, offsets per field row, as caused by non-immersion hood effect, for example the stages, are taken out.

Second, together with the improvements as shown in Figure 3 and other improvements not mentioned in this document, the improved thermal control leads to the following Single Machine Overlay:

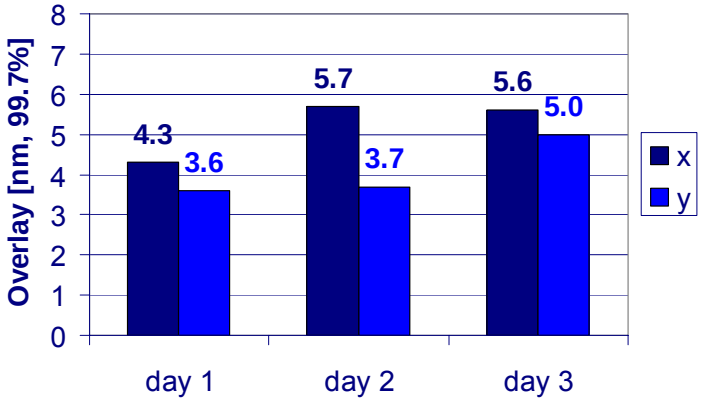

Figure 17. Single Machine Overlay (including both wafer stages).

The thermal control is further demonstrated in the so-called Reversed Overlay Test, see Figure 18. In this sensitive Overlay test, the first layer of a number of wafers is exposed in the normal sequence and the second layer is exposed in the reversed other. Any thermal instability, or other drifts, in time will become visible in the first and last wafer of this test.

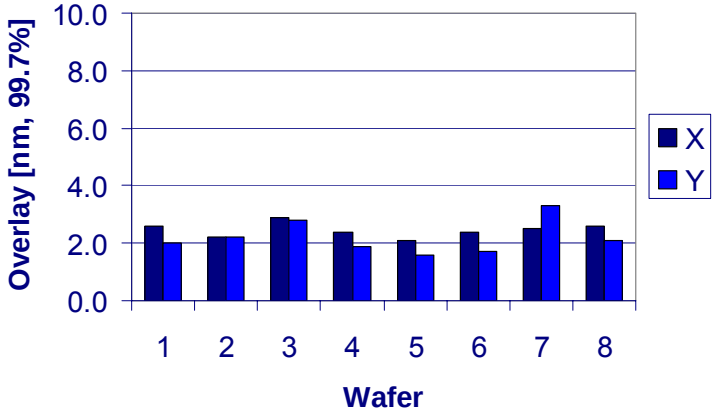

Figure 18. Reversed Dedicated Chuck Overlay with a full lot performance of 2.6 and 2.7nm in X and Y, resp..

Since no difference is visible between the first/last wafer and the middle wafers, the system is very stable.

Not only the inner fields show a good Overlay performance but the edge fields as well as enabled by the uniform wafer temperature distribution of Figure 11:

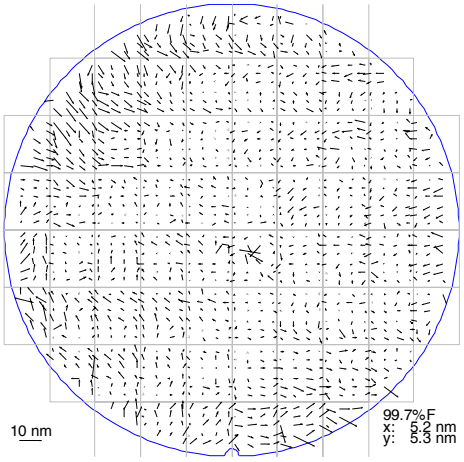

Figure 19. Full wafer Overlay <5.5nm.

The final result that proves the excellent thermal control is shown in Figure 20. In this test, time delays are inserted between wafers:

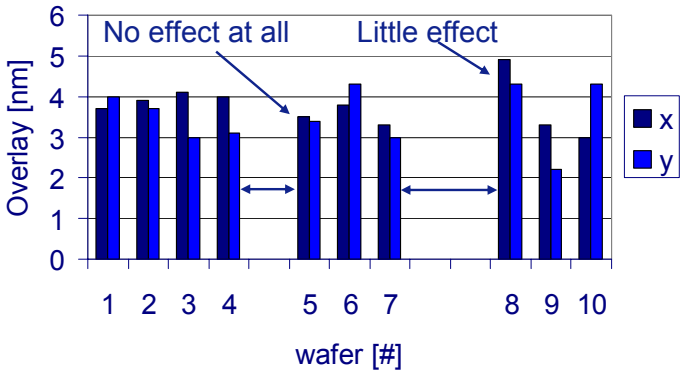

Figure 20. Overlay results with injected time delays of 43s (left arrow) and 89s (right arrow).

The stable results mean that wafer timing delays in the order of one minute, as caused by wafer track delays, have no effect on overlay.

The last Overlay result is presented in the following Figure where the XT:1900i is matched to a (dry) XT:1400 machine.

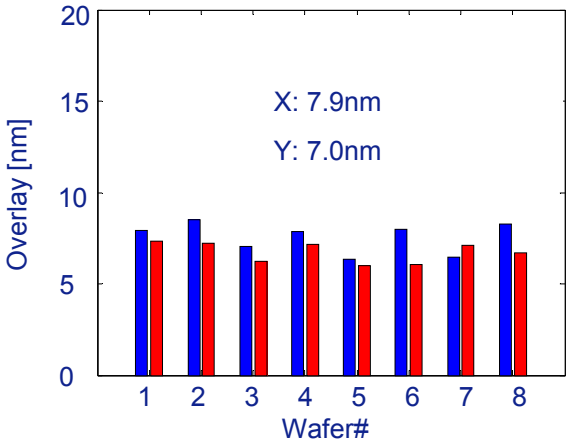

Figure 21. Overlay matching data between the XT:1900i and a (dry) XT:1400.

3.6. Throughput

The result of the throughput measurement is shown in the following Figure.

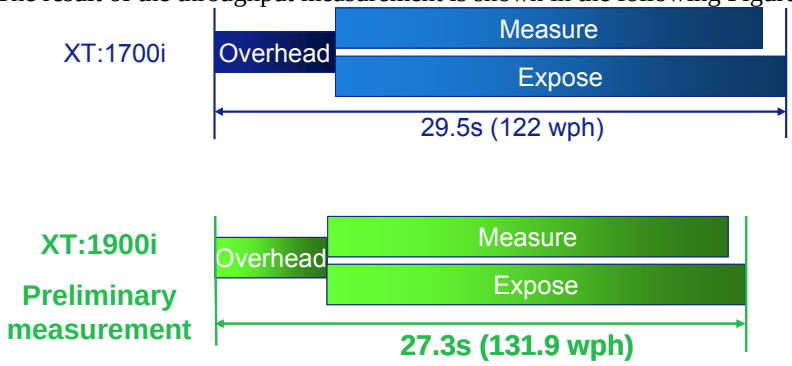

Figure 22. Faster stages increase the throughput from 122 to 131 wafers per hour.

4. Conclusions

- A resolution of 36.5nm half pitch in resist is demonstrated with the NA=1.35 projection lens
- The catadioptric lens concept is proven with manufacturing and volume ramp up capability
- The system has excellent Overlay, Focus, Imaging and Defectivity performance at 131 wph Throughput
- This performance supports volume production at 40nm resolution and below

ACKOWLEDEMENTS

The authors would like to thank all the members of the project team both at ASML and Carl Zeiss. Special thanks to the following people: Mark van de Kerkhof, Siebe Landheer, Martijn Leenders, William Whitty, Jan Mulkens, Mark Zellenrath, Anko Sijben, Raf Stegen, Menno Fien, Peter Krabbedam, Peter Smits, Marcel Beckers, Frank Spanjers, Andre Engelen, Gert Streutker, Oscar Noordman, Mark Trentelman, Peter Schrap, Tosca Kolen, Michael Thier, Markus Weber, Pieter Kramer, Martijn Kamphuis.

Part of the work was performed in the frame of the European EUREKA cluster program MEDEA+ and was financially supported by the Dutch Ministry of Economic Affairs and by the German Ministry of Education and Research.

REFERENCES

[1] H. Jasper et.al., *Immersion lithography with an ultrahigh-NA in-line catadioptric lens and a high-transmission flexible polarization illumination system*, SPIE 2006

[2] E. van Setten et. al., *Pushing the boundary: low-k1 extension by polarized illumination*, SPIE 2007, Vol 6520
[3] J. Mulkens et.al., *Defects, overlay and focus performance improvements with five generations of immersion exposure tools*, SPIE 2007, Vol. 6520